Unsupervised Myocontrol of a Virtual Hand Based on a Coadaptive Abstract Motor Mapping

Andrea Gigli[1,2], Arjan Gijsberts[3] and Claudio Castellini[1,2]

***Abstract*— Applications of simultaneous and proportional control for upper-limb prostheses typically rely on supervised machine learning to map muscle activations to prosthesis movements. This scheme often poses problems for individuals with limb differences, as they may not be able to reliably reproduce the training activations required to construct a natural motor mapping. We propose an unsupervised myocontrol paradigm that eliminates the need for labeled data by mapping the most salient muscle synergies in arbitrary order to a number of predefined prosthesis actions. The paradigm is coadaptive, in the sense that while the user learns to control the system via interaction, the system continually refines the identification of the user's muscular synergies. Our evaluation consisted of eight subjects without limb-loss performing target achievement control tasks of four actions of the hand and wrist. The subjects achieved comparable performance using the proposed unsupervised myocontrol paradigm and a supervised benchmark method, despite reporting increased mental load with the former.**

I. Introduction

Simultaneous and proportional (SP) myocontrol represents a promising methodology to control dexterous prosthetic hands naturally and intuitively. In this paradigm, regression models map muscular contractions directly to continuous motor commands for the degrees of freedom (DoFs) of the prosthesis [1]. The models are typically obtained via supervised machine learning, in which muscular data acquired from the subject's forearm is associated during a training phase with the desired motor commands.

Producing accurately labeled data can be challenging, especially for subjects with limb differences who stand to gain the most from this technology. Their impairment not only poses difficulties in precisely reproducing specific muscular activations, but also makes it impossible to verify whether the activations they produce actually correspond to the desired motor commands. Standard labeling protocols, therefore, resort to collecting labels using the contralateral hand as guidance or by pairing the desired motor commands with a visual stimulus [2]. These procedures typically require supervision from trained clinicians, are time-consuming, and are often perceived as mentally demanding by the target users.

A form of myocontrol that can learn motor mappings without labeled training data would be a desirable alternative to standard supervised myocontrol (SM). Existing approaches to such unsupervised myocontrol (UM) build upon evidence that the human motor system produces movements by jointly activating groups of muscles [3]. These muscle synergies function as high-level motor commands that can be combined to produce more fine-grained motor control. Lin et al. [4] achieved quasi-unsupervised myocontrol of the DoFs of the wrist through a principled calibration protocol. First, they collected unlabeled calibration surface electromyography (sEMG) by asking the subjects to selectively move the desired DoFs of the wrist. Then, they used a nonnegative matrix factorization (NMF) algorithm with sparsity constraints to express the calibration sEMG as the activity of minimally-overlapping muscle synergies. Finally, they assigned muscle synergies to DoFs by observing which synergy was most active while activating each DoF. The work by Yeung et al. [5] extends the calibration procedure described above, accounting for the evolution of muscle synergies over time due to the subject's familiarization with the myocontrol system and the displacement of electrodes, among other factors. They accommodate for those changes by employing an adaptive version of NMF with sparsity constraints and a forgetting mechanism that progressively discounts the contribution of old input samples. The method automatically triggers unsupervised model updates when model degradation is detected during normal operation. Both approaches allowed performance comparable to a SM benchmark in target-reaching tasks involving a cursor on a screen.

The semi-unsupervised calibration procedure used by the previous works requires subjects to repeat the same muscular activations in an open-loop. This is done so that an individual synergy can be isolated and mapped to the DoF of the prosthesis that physiologically corresponds to the muscular activation. As mentioned, this can be unpractical for subjects with limb differences, who may not be able to precisely and repeatably control each DoF of their phantom limb. In these cases, it would be preferable to control hand movements via an abstract motor mapping, that is, by muscular activations that may not be physiologically related to those movements. In this manner, subjects could control their prosthesis using the muscular patterns that they can elicit best.

Numerous works on motor learning have demonstrated the human capacity to learn abstract motor mappings through closed-loop interaction with a myocontrol system [6]. Ison and Artemiadis [7] demonstrated that humans can learn non-trivial motor mappings between the combined activity of biomechanically independent muscles and the position of a cursor on a screen. Their research also showed that the

[1] Institute of Robotics and Mechatronics, German Aerospace Center (DLR), 82234 Weßling, Germany. name.surname@dlr.de

[2] Chair of Medical Robotics, Friedrich-Alexander University Erlangen-Nuremberg, 91054 Erlangen, Germany

[3] Unaffiliated

learned motor skills are retained over time and can generalize to different myocontrol tasks, such as controlling the position of a robot's end-effector on a plane. Pistohl et al. [8] showed that abstract motor mappings can be effectively used to control myoelectric hands. Their approach arbitrarily maps the activity of a specific muscle to the control of an action of the hand and relies on the subject to learn to use that mapping. However, this motor learning may be complicated if the muscles used in the motor mapping are biomechanically coupled [9], as is the case in the human forearm. To control myoelectric hands it may thus be advantageous to define abstract motor mappings based on automatically extracted muscle synergies rather than individual muscle activations.

In this work, we introduce a novel coadaptive UM paradigm that integrates incremental extraction of muscle synergies and adaptation to an abstract motor mapping that is based on those synergies. The system adaptively decomposes muscular control inputs into sparse muscle synergies using a purposedly designed incremental NMF algorithm with sparsity constraints and a forgetting mechanism to discount the contribution of old input samples. Although derived independently, our formulation is similar (but not equal) to the NMF algorithm used by Yeung et al. [5], which was published during our paper's final redaction. In contrast to their approach, this algorithm is used to implement an abstract motor mapping between the synergies' activations and a set of desired actions of the hand or wrist that may not be physiologically related to those activations. A virtual hand on a monitor visualizes the model's prediction in real-time and closes the control loop with the subject. Subjects are instructed to learn to perform the desired actions with the virtual hand, starting from eliciting arbitrary muscular contractions. This paradigm involves coadaptation between subjects and myocontrol model. Subjects aim to elicit more distinctive muscular patterns whilst the model incrementally decomposes those patterns into sparse muscle synergies. Conveniently, this paradigm does not require any initial calibration of the myocontrol system, is easily understood by the subjects, and encourages them to explore their muscular space to identify distinctive muscular patterns for myocontrol. We compare the proposed UM paradigm to a state-of-the-art SM in a series of target achievement control (TAC) tests and via a questionnaire.

The remainder of this paper is organized as follows. In section II, we describe our UM method and its experimental evaluation. The corresponding results are then described in section III. A discussion of the results follows in section IV and the paper is concluded in section V.

II. Materials and Methods

A. Coadaptive unsupervised myocontrol paradigm

We present a UM paradigm that adaptively extracts sparse muscle synergies, implements an abstract motor mapping based on those synergies, and leverages closed-loop adaptation to that mapping. Figure 1 provides an overview of this paradigm. The resulting myocontrol model uses the activation of the detected muscle synergies to control an arbitrary set of actions of the hand and wrist simultaneously and proportionally.

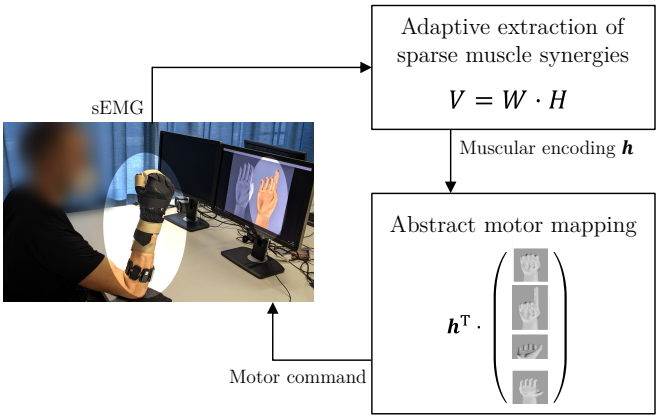

Fig. 1: *Proposed unsupervised myocontrol paradigm (UM).* While the subjects learn to control the artificial hand by interacting with the system, their muscular activity is adaptively decomposed in sparse muscle synergies. The activation levels of these synergies are used to activate a predefined set of hand actions based on an abstract motor mapping. The detected control action is fed back to the user via a skin-colored hand on a monitor. During the TAC tasks, the subject has to match the target action of the hand shown in gray on the monitor.

Incremental extraction of sparse muscle synergies: Because the subjects' adaptation to the myocontrol model causes changes in their muscular synergies, we require a factorization algorithm that can incrementally extract and update the decomposition of the input signals. To this end, we formulate incremental sparse nonnegative matrix factorization (ISNMF) with forgetting, which is an incremental version of NMF with additional sparsity constraints and a mechanism to discount the contribution of old input samples.

Standard NMF decomposes a nonnegative data matrix $\boldsymbol{V}$ of s n-dimensional samples as $\boldsymbol{V} \approx \boldsymbol{W}\boldsymbol{H}$, where factors $\boldsymbol{W}$ and $\boldsymbol{H}$ are restricted to be nonnegative. The $n \times r$ matrix $\boldsymbol{W}$ contains the basis vectors, whereas the $r \times s$ encoding matrix $\boldsymbol{H}$ contains for each sample the activations of the bases as to reconstruct $\boldsymbol{V}$ as accurately as possible.

This problem can be solved incrementally by updating the bases and encoding matrices when new data becomes available. At the m-th update, the old data matrix $\boldsymbol{V} = \begin{bmatrix}\boldsymbol{V}^1 & \cdots & \boldsymbol{V}^{m-1}\end{bmatrix}$ is extended with the new data samples $\boldsymbol{V}^m$, and the encoding matrix $\boldsymbol{H} = \begin{bmatrix}\boldsymbol{H}^1 & \cdots & \boldsymbol{H}^{m-1}\end{bmatrix}$ is extended with randomly initialized encoding coefficients $\boldsymbol{H}^m$. The basis matrix $\boldsymbol{W}^m$ and the new encoding coefficients $\boldsymbol{H}^m$ can then be found by minimizing the objective function

$$F^m = \frac{1}{2}\sum_{j=1}^{m} \mu^{m-j} \left\| \boldsymbol{V}^j - \boldsymbol{W}^m \boldsymbol{H}^j \right\|_F^2 + \gamma \sum_{j=1}^{m} \mu^{m-j} \left\| \boldsymbol{H}^j \right\|_1 + \frac{\beta}{2} \left\| \boldsymbol{W}^m \right\|_F^2 , \qquad (1)$$

where $\mu \in (0, 1]$ is a forgetting factor that exponentially discounts old input samples, and $\beta \geq 0$ and $\gamma \geq 0$ determine the regularization strength for the encoding and the basis

matrices. With $\|\cdot\|_F$ and $\|\cdot\|_1$ we denote the Frobenius and the elementwise L_1 norms. Furthermore, we assume that the former encoding blocks $\boldsymbol{H}^1$ to $\boldsymbol{H}^{m-1}$ would not change much and therefore do not optimize these. This approximation constrains the number of parameters that need to be optimized at each update and has other computational benefits [10, 11].

The problem can be solved incrementally following the procedure in algorithm 1 based on multiplicative updates, analogous to the derivation presented in other related work [10, 11]. Model updates are performed in constant time and memory by storing the model state into constant-sized history matrices instead of retaining old data samples. Encodings of new data samples in the updated synergy space can be obtained by repeatedly applying the rule on line 17. Among the algorithm's hyperparameters, r represents the desired number of NMF components, while the tolerance $\epsilon > 0$ and the maximum number of iterations $t_{\max} > 0$ are used for the stopping condition of the iterative optimization. The elements of $\boldsymbol{W}^1$ and $\boldsymbol{H}^m$ are initialized randomly to $\max(0, \mathcal{N}(\bar{\boldsymbol{V}}^m, 1))$, with $\bar{\boldsymbol{V}}^m$ being the average value of the new data samples and $\mathcal{N}$ representing the normal distribution. Subscripts ij indicate the element at the i-th row and the j-th column of the corresponding matrix.

Algorithm 1: ISNMF

Input: stream $\mathcal{S}$ of n-dim nonnegative samples
Parameters: r, β, γ, μ, ϵ, $t_{\max}$

1 $m \leftarrow 0$
2 $\boldsymbol{A} \leftarrow [0]_{n \times r}$
3 $\boldsymbol{B} \leftarrow [0]_{r \times r}$
4 **while** *true* **do**
5 $\quad m \leftarrow m + 1$
6 $\quad \boldsymbol{V}^m \leftarrow n \times k$ matrix with k new samples from $\mathcal{S}$
7 $\quad$ **if** $m = 1$ **then**
8 $\quad\quad \boldsymbol{W}^m \leftarrow n \times r$ strictly positive random matrix
9 $\quad$ **else**
10 $\quad\quad \boldsymbol{W}^m \leftarrow \boldsymbol{W}^{m-1}$
11 $\quad$ **end**
12 $\quad \boldsymbol{H}^m \leftarrow r \times k$ strictly positive random matrix
13 $\quad e_0 \leftarrow \|\boldsymbol{V}^m - \boldsymbol{W}^m \boldsymbol{H}^m\|_F^2$
14 $\quad t \leftarrow 0$
15 $\quad$ **repeat**
16 $\quad\quad t \leftarrow t + 1$
17 $\quad\quad \boldsymbol{H}^m_{ij} \leftarrow \boldsymbol{H}^m_{ij} \frac{(\boldsymbol{W}^{m\intercal} \boldsymbol{V}^m)_{ij}}{(\boldsymbol{W}^{m\intercal} \boldsymbol{W}^m \boldsymbol{H}^m)_{ij} + \gamma \operatorname{sgn}(\boldsymbol{H}^m_{ij})}$
18 $\quad\quad \boldsymbol{W}^m_{ij} \leftarrow \boldsymbol{W}^m_{ij} \frac{(\mu \boldsymbol{A} + \boldsymbol{V}^m \boldsymbol{H}^{m\intercal})_{ij}}{(\mu \boldsymbol{W}^m \boldsymbol{B} + \boldsymbol{W}^m \boldsymbol{H}^m \boldsymbol{H}^{m\intercal} + \beta \boldsymbol{W}^m)_{ij}}$
19 $\quad\quad e_t \leftarrow \|\boldsymbol{V}^m - \boldsymbol{W}^m \boldsymbol{H}^m\|_F^2$
20 $\quad$ **until** $|e_t - e_{t-1}|/e_0 < \epsilon$ **or** $t > t_{max}$
21 $\quad \boldsymbol{A} \leftarrow \mu \boldsymbol{A} + \boldsymbol{V}^m \boldsymbol{H}^{m\intercal}$
22 $\quad \boldsymbol{B} \leftarrow \mu \boldsymbol{B} + \boldsymbol{H}^m \boldsymbol{H}^{m\intercal}$
23 **end**

Adaptive abstract motor mapping: The proposed UM system periodically computes the encoding of a new muscular input and regards its components as primitive motor commands. These components are normalized to the range $[0, 1]$ by dividing them by their historical 95-th percentile computed incrementally and bounded above by 1. Each of the resulting control signals is associated with one of a predefined set of hand actions, where the order depends on the random initialization of $\boldsymbol{W}^1$ and the subsequent incremental updates. We refer to this association as an abstract motor mapping, because it is not based on a physiological correspondence between muscle activity and action of the hand. Since multiple control signals may be nonzero at the same time, this allows simultaneous and proportional control of the hand.

Adaptation to the motor mapping: The control loop is closed by rendering the predicted action on a virtual hand on a screen in real-time. Subjects are induced to learn the abstract motor mapping implemented by the myocontrol model through simple instructions. First, they are told which basic actions the virtual hand can perform. Second, they are informed that those actions can be controlled by performing possibly different actions with their own (phantom) limb. Finally, they are asked to identify which actions of their hand precisely control the basic actions of the virtual hand, starting by performing random actions and observing the virtual hand's reaction. The proposed myocontrol paradigm is coadaptive because subjects and myocontrol model synergistically try to generate distinctive muscular commands and adaptively discriminate sparse muscle synergies from them.

B. Experiment: evaluation of unsupervised myocontrol

We compared the proposed unsupervised myocontrol approach to a state-of-the-art supervised one in a series of TAC tests.

Participants: Eight non-disabled subjects participated in the experiment. The study was conducted at the German Aerospace Center according to the WMA Declaration of Helsinki and approved by the Institution's internal committee for personal data protection.

Experiment setup: One Myo armband by Thalmic Labs provided 200 Hz 8-channels sEMG measurements of the forearm muscles of the subjects' right arm. Limbs movements were restricted by padding the hand with two thick gloves and securing the limb to an orthotic splint of the hand and wrist. Moreover, subjects were asked to lay their elbow on a table before them and to avoid rotating their wrist during the experiment. A monitor displayed a skin-colored virtual hand that showed the myocontrol model's prediction in real-time and a gray hand that provided reference actions during the experiment. The experimental setup can be seen in Figure 1.

Data processing and myoelectric control: The stream of sEMG measurements was band-pass filtered online using a second-order Butterworth filter with cutoff frequencies of 10 Hz and 90 Hz. Then, the envelope of each channel was computed as the root mean square of the signal over the last 200 ms and used as input signal for both tested myocontrol paradigms.

Four basic actions of the hand and wrist were selected for myocontrol in this experiment. They were a power grasp, a pointing with the index finger, a wrist flexion, and a wrist extension. The number of basic actions corresponded with the maximum number of distinct muscle synergies that could be extracted reliably from the sEMG data measured with our setup. The actions were chosen based on their relevance in activities of daily living and because they are challenging in realistic myocontrol settings.

Based on preliminary tests, the hyperparameters of the ISNMF algorithm were set to $r = 4$, $\beta = \gamma = 30$, $\mu = 0.95$, $\epsilon = 1e-5$, and $t_{\text{max}} = 200$. The synergy model was updated at $f_u = 0.2\,\text{Hz}$ using the k samples available from the previous update. New encodings were computed at $f_p = 20\,\text{Hz}$ and used to predict the desired action.

We compared UM to an existing supervised SM approach that uses ridge regression with random Fourier features (RFFRR). This approach, based on nonlinear regression, provided state-of-the-art performance in a variety of SP myocontrol applications including prosthetic control [12]. The interested reader is referred to [12] for details about the method. We set the bandwidth and dimensionality of the RFF mapping respectively to 1 and 300, the regularization parameter of the regressor to 1, and the prediction frequency to $f_p = 20\,\text{Hz}$.

C. Experiment protocol

All subjects tested both UM and SM, in randomized order, performing two types of exercises. The first type was aimed at updating the myocontrol models, and denoted as coadaptation round for UM or calibration round for SM. The second type consisted of TAC tasks aimed at testing the models. For each condition, three coadaptation or calibration rounds were alternated with three TAC tests involving basic actions to allow subjects to reach comparable familiarization with the system; two TAC tests involving combinations of basic actions concluded the sequence of exercises. In the following, we will refer to the coadaptation (for UM) or calibration (for SM) rounds as C, to the TAC tests on basic actions as TB, and to the TAC tests on combined actions as TC. The sequence of exercises performed by the subjects for both UM and SM was, therefore: C1, TB1, C2, TB2, C3, TB3, TC1, TC2.

The unsupervised model was randomly initialized at the beginning of the experiment and progressively updated throughout the following coadaptation rounds. They consisted of 300 s long sessions allocated for the UM model to update the abstract motor mapping and for the subject to adapt to it. The supervised model was initialized to provide null predictions and updated in the subsequent calibration rounds. In each calibration round, labeled training data was obtained while asking subjects to hold each basic action and a resting hand gesture for 5 s. The model could be updated with more training data for the actions that were deemed not controllable.

In the TAC tasks, the myocontrolled virtual hand had to be matched with the target action displayed by the reference virtual hand. A task would be considered successful if the subject managed to keep the predicted DoFs within a euclidean distance of $d \leq 0.15$ from the target action for at least a continuous 1 s before the 10 s maximum task duration. During the TAC tests, the automatic updates of the unsupervised model were suspended for better comparability with the supervised strategy. The same TAC tests were performed for both conditions. The TAC tests involving basic actions included 16 tasks, corresponding to the four basic actions presented at two intensity levels, 50 % and 100 %, and repeated twice in random order. Those involving combined actions included eight tasks, corresponding to the four possible combinations of basic actions of the hand and the wrist, repeated twice in random order.

D. Performance evaluation

The performances achieved by UM and SM in the TAC tests were compared based on standard metrics. Success rate (SR) is the percentage of successful tasks in one TAC, time to complete the task (TCT) is the time to successfully complete one task, number of overshoots (NO) is the number of times the predicted actions approached the target and then moved away from it, mean error in target (MET) is the average euclidean distance between predicted and target action after reaching the target for the first time, and path efficiency (PE) is the ratio between the length of the optimal path and the predicted path from the rest action to the target action.

Moreover, subjects self-assessed performance of the myocontrol models at the end of each TAC in terms of mental effort, physical effort, and frustration. The ratings were reported on visual analog scales (VASs) ranging from "low", corresponding to 0 %, to "high", corresponding to 100 %. Subjects also assessed their satisfaction with the coadaptation rounds of UM in terms of mental effort, physical effort, and frustration level in the same questionnaire. As this is an initial study on the proposed UM paradigm with a limited number of subjects, we lack the statistical power for meaningful significance tests and instead report the individual data points when possible.

III. Experimental Results

Figure 2(a) shows the success rate achieved during each TAC test. Subjects reached comparable success rates around 50 % with UM and SM in all TAC tests involving basic actions. Controlling combined hand actions proved considerably more difficult, especially with SM. Only one subject managed to complete about 10 % of the combined actions with SM, while approximately half the subjects obtained success rates between 10 % to 50 % with UM. This discrepancy may have to do with the fact that the linear ISNMF method interpolates more predictably than RFFRR in parts of the input space that were unseen during the training phase. The comparison between UM and SM is not investigated further due to the very lacking performance of the latter.

Figure 2(b-e) focuses on the tasks on basic actions that were completed successfully and characterizes how quickly and accurately they were executed. Trends of the median

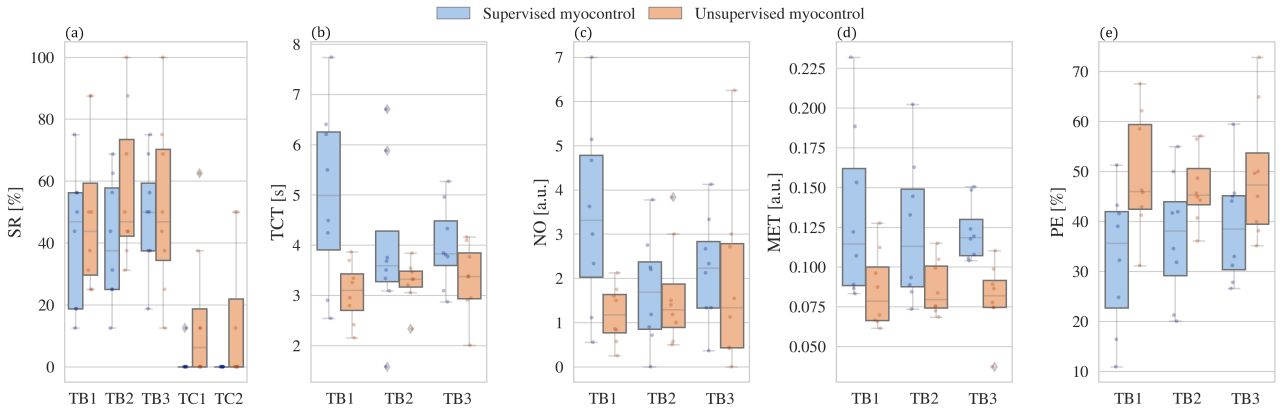

Fig. 2: *Myocontrol performance in the TAC tests.* (a) Success rate achieved during the TAC tests. (b-e) Performance achieved in tasks on basic actions that were completed successfully. Each of the points displayed within the boxplots represents the average of a statistic achieved by one subject during the tasks of the corresponding TAC.

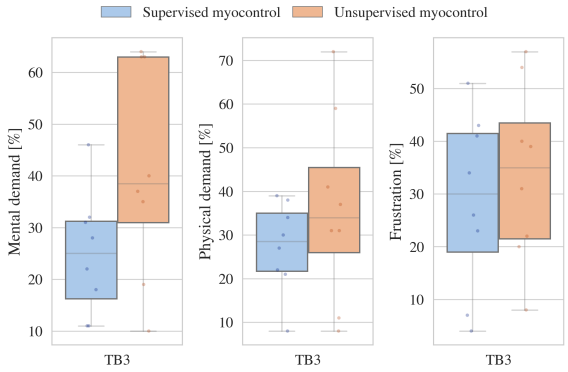

Fig. 3: *Self-assessed myocontrol performance.* Mental and physical demand, and frustration with the myocontrol model during the last TAC on basic actions, TB3.

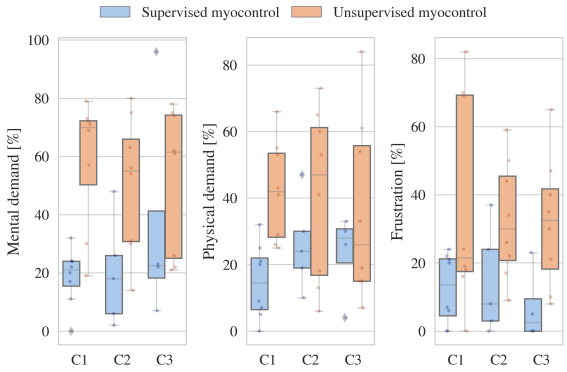

Fig. 4: *Questionnaire unsupervised coadaptation rounds.* Mental and physical demand, and frustration level related to the calibration rounds of SM and the coadaptation rounds of UM.

value and the spread of every metric suggest that subjects familiarized themselves with SM during the first TAC test and reached comparable performance to UM during the following ones. Presumably, a similar familiarization effect was not observed for UM because subjects had gained proficiency with the system already during the first coadaptation phase. During the last TAC test on basic actions, TB3, subjects completed the tasks in about 3.5 s with either myocontrol paradigm. On average, each target action was overshot two times with SM and one time with UM, indicating that the latter allowed slightly better control while approaching the target action. Nevertheless, the magnitude of the overshoots was small for both approaches. The median value of the MET, around 0.012 for SM and 0.08 for UM, was only about 5 % of the maximum possible MET. A median path efficiency around 40 % for SM and 50 % for UM, indicates that target actions were reached with comparably efficient movements. The small difference in path efficiency reflects the slightly more frequent overshoots with SM.

Despite performing equivalently well with either myocontrol paradigm, subjects deemed UM more mentally challenging, as shown in Figure 3. Most subjects reported mental loads between 10 % and 30 % for SM and between 30 % and 60 % for UM. Nonetheless, the level of physical effort and frustration with the myocontrol system were more comparable for the two approaches.

Figure 4 characterizes the coadaptation rounds of UM in terms of mental demand, physical demand, and overall frustration level, as compared to the standard calibration procedure used for SM. Most subjects found coadaptation rounds considerably more mentally challenging than calibration rounds. The physical demand and frustration levels were also slightly higher for the coadaptive procedure. These results could be explained by the subjects having to learn new abstract motor mappings, the longer duration of the calibration procedure, or the model adaptation not fully meeting the subjects' expectations.

IV. Discussion

The results of our experiment show that subjects can learn abstract motor mappings controlled by sparse muscle synergies extracted online. By the end of the first coadaptation round, most subjects had managed to control all the basic

actions of the virtual hand independently. This indicates that the ISNMF algorithm adaptively identified a set of muscle synergies in the input signals that were distinctive enough to control the virtual hand's basic actions precisely. It also confirms that subjects quickly learned the abstract motor mapping implemented by the myocontrol algorithm, i.e., they identified which actions of their restricted hand controlled the desired actions of the virtual hand.

We note that our coadaptive UM paradigm induced subjects to autonomously, and perhaps subconsciously, explore their own muscular space. This could be especially beneficial for individuals with limb differences, allowing them to independently discover muscular activations that they can elicit comfortably and repeatably enough for use in myoelectric control. In future work, we hope to experimentally confirm these benefits for individuals with limb differences.

Some subjects complained about not being able to control one of the virtual actions independently of the others, despite trying numerous control inputs. This is reflected in the non-decreasing frustration about the coadaptation phase reported in the questionnaire (Figure 4). We argue that this problem relates to adopting a unique set of hyperparameters for the ISNMF algorithm for all the subjects. Although they had been optimized on preliminary tests, stronger regularization and forgetting could have been helpful for some subjects. Future investigation will include strategies to automatically tune those hyperparameters during the experiment based on codependencies between the extracted muscle synergies.

Our experiment also shows that abstract motor mappings based on adaptively extracted muscle synergies enable fully unsupervised SP myocontrol of artificial hands. The approach performed equivalently well as state of the art SM with a physiologically-inspired motor mapping (Figure 2), and the two paradigms generated comparable frustration levels in the subjects (Figure 3). Nonetheless, the mental effort required for UM was higher than for SM (Figure 3). Presumably, this is because all subjects were non-disabled; they had to learn the abstract motor mappings used in UM while they were already familiar with the physiologically-inspired mapping used in SM. We would expect to see higher levels of mental effort for subjects with limb differences when using SM.

V. Conclusions

To avoid the need for labeled training data for simultaneous and proportional myocontrol, we proposed an unsupervised and coadaptive myocontrol paradigm. Our myocontrol system incrementally refines the recognition of sparse muscle synergies from sEMG measurements and maps them arbitrarily to a set of hand actions. At the same time, the user interacts with the system in a closed-loop and learns to control this abstract motor mapping by producing more distinctive muscular patterns. In a series of TAC tests with eight non-disabled subjects, this unsupervised myocontrol paradigm performed as well as a supervised reference method in terms of task success rate, completion time, and path efficiency, despite coming at a higher self-reported mental load. This demonstrates the capacity of humans to learn to control abstract motor mappings based on adaptively extracted muscle synergies and supports the feasibility of using the proposed UM paradigm for prosthetic control.

Acknowledgements

This work was partially supported by the DFG project Deep-Hand, CA1389/1-2. The authors would like to thank the participants in the user study and Mr. Markus Nowak for his insightful feedback on the experimental protocol.

References

[1] A. Fougner, Ø. Stavdahl, P. J. Kyberd, Y. G. Losier, and P. A. Parker, "Control of upper limb prostheses: Terminology and proportional myoelectric control—a review," *IEEE Transactions on neural systems and rehabilitation engineering*, vol. 20, no. 5, pp. 663–677, 2012.

[2] A. Hagengruber, U. Leipscher, B. M. Eskofier, and J. Vogel, "A new labeling approach for proportional electromyographic control," *Sensors*, vol. 22, no. 4, p. 1368, 2022.

[3] M. Santello, G. Baud-Bovy, and H. Jörntell, "Neural bases of hand synergies," *Frontiers in Computational Neuroscience*, vol. 7, 2013.

[4] C. Lin, B. Wang, N. Jiang, and D. Farina, "Robust extraction of basis functions for simultaneous and proportional myoelectric control via sparse non-negative matrix factorization," *Journal of neural engineering*, vol. 15, no. 2, p. 026017, 2018.

[5] D. Yeung, I. M. Guerra, I. Barner-Rasmussen, E. Siponen, D. Farina, and I. Vujaklija, "Co-adaptive control of bionic limbs via unsupervised adaptation of muscle synergies," *IEEE Transactions on Biomedical Engineering*, 2022.

[6] M. Ison and P. Artemiadis, "The role of muscle synergies in myoelectric control: trends and challenges for simultaneous multifunction control," *Journal of neural engineering*, vol. 11, no. 5, p. 051001, 2014.

[7] M. Ison and P. Artemiadis, "Proportional myoelectric control of robots: muscle synergy development drives performance enhancement, retainment, and generalization," *IEEE Transactions on Robotics*, vol. 31, no. 2, pp. 259–268, 2015.

[8] T. Pistohl, C. Cipriani, A. Jackson, and K. Nazarpour, "Abstract and proportional myoelectric control for multi-fingered hand prostheses," *Annals of biomedical engineering*, vol. 41, no. 12, pp. 2687–2698, 2013.

[9] A. De Rugy, G. E. Loeb, and T. J. Carroll, "Muscle coordination is habitual rather than optimal," *Journal of Neuroscience*, vol. 32, no. 21, pp. 7384–7391, 2012.

[10] S. S. Bucak and B. Gunsel, "Incremental subspace learning via non-negative matrix factorization," *Pattern recognition*, vol. 42, no. 5, pp. 788–797, 2009.

[11] S. Dang, Z. Cui, Z. Cao, and N. Liu, "Sar target recognition via incremental nonnegative matrix factorization," *Remote Sensing*, vol. 10, no. 3, p. 374, 2018.

[12] A. Gigli, A. Gijsberts, and C. Castellini, "The merits of dynamic data acquisition for realistic myocontrol," *Frontiers in Bioengineering and Biotechnology*, 2020.